International Journal of Biological Macromolecules 282 (2024) 136648

Contents lists available at ScienceDirect

International Journal of Biological Macromolecules

journal homepage: www.elsevier.com/locate/ijbiomac

Heparin-functionalized Cu-based metal-organic framework: An efficient active and passive targeting nanocarrier for anticancer doxorubicin drug delivery

Sima Darvishi [a], Hossein Hosseinzadeh [b], Fahimeh Kazeminava [c], Amin Mahoutforoush [c], Mohammadreza Tajik [d], Monireh Rasoulzadehzali [c], Reza Mohammadi [b,*], Samaheh Sadjadi [e,**], Siamak Javanbakht [b,*]

[a] Department of Chemistry, School of Physic and Chemistry, Alzahra University, PO Box 1993891176, Vanak, Tehran, Iran
[b] Polymer Research Laboratory, Department of Organic and Biochemistry, Faculty of Chemistry, University of Tabriz, Tabriz, Iran
[c] Drug Applied Research Center, Tabriz University of Medical Sciences, Tabriz, Iran
[d] Department of Biomedical Engineering, Carnegie Mellon University, Pittsburgh, USA
[e] Gas Conversion Department, Faculty of Petrochemicals, Iran Polymer and Petrochemical Institute, PO Box 14975-112, Tehran, Iran

ARTICLE INFO

Keywords:
Metal-organic framework
Heparin
Doxorubicin
Drug delivery
Receptor

ABSTRACT

In this study, by innovative combining the unique characteristics of Cu-based metal-organic framework (MOF) with the versatile attributes of saccharides (i.e., heparin, Hep), a promising approach is established for active and passive targeting DDS, Cu-MOF/Hep, with a pH-controlled release profile and enhanced drug efficacy. The characterization of the synthesized materials (i.e., FT-IR, XRD, SEM, EDX, TEM, DLS, and TGA) confirms the successful synthesis of Cu-MOF/Hep. In vitro studies concerning the loading and release of DOX observed that a higher amount of DOX was released at pH 5 (>90 % on 96 h, 41 °C) compared to pH 7.4 (<10 % on 96 h, 37 °C). The sensitive feature of the used MOF to the pH conditions increased the drug release in environmental conditions similar to cancer tissues. Furthermore, cytotoxicity assessments indicated notable cytotoxicity effects of DOX-loaded Cu-MOF/Hep on MCF-7 cells (IC_{50}: ~10 μg/mL in 48 h) with a significant apoptosis rate. The existence of CD44 receptors on the surfaces of cells underscores the significance of Hep-modified systems in facilitating the apoptosis of cancerous cells. The results suggest that the combined Cu-MOF and Hep have the potential to be a viable option for creating platforms that deliver anticancer treatments.

1. Introduction

Annually, a significant number of individuals die of cancer across the world [1]. Hence, cancer is an intricate disease that has been a prominent subject of medical investigation for a considerable period [2,3]. The primary conventional approaches to treating cancer include surgical procedures [4], chemotherapy [5], and radiation therapy, aimed at eliminating, reducing, or eradicating cancerous cells [6]. Nonetheless, these treatments are accompanied by drawbacks and side effects, such as the development of drug resistance in chemotherapy and harm to healthy cells in radiation therapy [7]. Targeted drug delivery is one of the ways to overcome the side effects of this method [8]. The purpose of using these systems is the targeted delivery of drugs to cancer tissues and the slow release of drugs in these tissues [9].

Recent research has presented a range of techniques and substances, especially in the nanoscale range, with distinct properties that can be utilized in drug delivery systems [10,11]. Recently, MOF structures due to their unique properties have become prominent materials in drug delivery applications [12]. MOFs are porous substances consisting of metal ions or clusters connected by organic ligands [13]. Their considerable surface area, pH-responsive, adjustable pore dimensions, and varied chemistry render them auspicious contenders for drug conveyance purposes [14]. MOFs can be engineered to encapsulate, drug store, and deliver therapeutic agents with controlled release profiles, targeted transportation to specific tissues, and enhanced drug endurance [15,16]. Their biocompatibility, versatility, and ability to overcome the

* Corresponding authors at: University of Tabriz, Tabriz, Iran.
** Correspondence to: S. Sadjadi, Iran Polymer and Petrochemical Institute, Tehran, Iran.
E-mail addresses: r.mohammadi@tabrizu.ac.ir (R. Mohammadi), s.sadjadi@ippi.ac.ir (S. Sadjadi), s_javanbakht@tabrizu.ac.ir (S. Javanbakht).

https://doi.org/10.1016/j.ijbiomac.2024.136648
Received 6 July 2024; Received in revised form 7 October 2024; Accepted 15 October 2024
Available online 20 October 2024

limitations of conventional drug delivery systems make MOFs a promising platform for enhancing the efficacy and safety of drug delivery in various medical treatments [17,18].

Hep, a commonly used anticoagulant, plays an essential role in enhancing the effectiveness and safety of various drug delivery systems [19]. Its distinct characteristics render it a versatile material in the stabilization of nanoparticles [20], controlling drug release [21], targeting specific cells or tissues, and enhancement of drug solubility [22]. This precise drug delivery strategy not only increases the efficiency of therapeutic medications but also reduces unintended impacts, thus improving the overall safety and efficacy of the treatment. The capability of Hep to facilitate targeted drug delivery establishes it as a valuable component in optimizing the accuracy and efficiency of drug therapies [23].

Cellular receptors, are proteins situated on the exterior of cells, engage with particular molecules in the extracellular milieu, prompting cellular reactions [24]. These receptors are integral in a range of physiological functions such as cellular growth, metabolism, signaling, and immune defense. The functionality of cellular receptors relies on their capacity to identify and attach to particular ligands, including hormones, neurotransmitters, growth factors, or other molecules [25]. Upon binding of a ligand to a receptor, biochemical signals are triggered within the cell, resulting in alterations in gene expression, protein activity, and cellular behavior [25]. The CD44 is a receptor that is located on the surface of cells and functions as attachment points for different ligands (i.e., Hep and hyaluronic acid) [25,26]. These receptors participate in a range of cellular activities such as cell adhesion, migration, proliferation, and signaling. Various kinds of Hep segments including syndecans, glypicans, and integrins are present on the surface of cells [27]. The CD44 receptor has distinct binding regions that interact with Hep and facilitate the entry of substances containing Hep into the cells [28]. In general, the presence of CD44 receptors on the cell surface plays an important role in the entry of substances containing Hep into the cell and its effect on various cellular processes and emphasizes the importance of Hep as an important polysaccharide in therapeutic strategies [29]. Hep-modified DDSs have demonstrated a strong ability to target cancer cells that overexpress the CD44 receptor, while also reducing the capture of drugs by the liver [30,31]. Importantly, heparin's mechanisms of action, including anti-inflammatory properties and cell adhesion modulation, operate independently of its anticoagulant effects. This distinction is crucial as it allows for the therapeutic use of heparin in DDSs without compromising the pharmacological efficacy of the delivered drugs. Past research has suggested that active targeting is more effective than passive targeting, indicating a shift towards this approach in the design of drug delivery systems [32,33].

Recently, our research team has explored and combined diverse MOF structures with saccharides, leading to the synthesis of various composites [34–36]. As far as we know, MOF structures based on Cu metal and modified with Hep have not been employed in such systems. Consequently, this study investigates a novel nanocomposite for use as active and passive targeting drug delivery systems. According to the literature [37–39], Cu (BDC) MOFs because of their pH-sensitive nature and positive charge value were chosen in the current study and modified with Hep to take advantage of their favorable characteristics including responsiveness to pH, porous structure, capacity for drug loading, ability to degrade in acidic environments, as well as their affinity for binding to cellular receptors. These modified MOFs were then examined for their potential application in active and passive targeting delivery of doxorubicin (DOX).

2. Experimental

2.1. Materials

Heparin sodium 5000 I.U./mL solution (Hep, Purity ≥97.0 %, $M_{w,0}$ ≈ 20,000 g/mol, $M_w/M_n = 1.1$, the average degree of sulphation: ~2.7 per disaccharide unit) was achieved from Sigma-Aldrich Co. Copper (II) nitrate trihydrate (Cu $(NO_3)_2.3H_2O$) (≥99 % purity), terephthalic acid (98 % purity), dimethylformamide (DMF) (99.8 % purity) were achieved from Merck KGaA Co. Doxorubicin hydrochloride (DOX) was obtained from Sobhan Pharmaceuticals (Iran). Acetone (≥99.5 % purity) was purchased from CARLO ERBA Reagents (S.A.S) and ethanol (EtOH) (96 % purity) was obtained from Pars Alcohol Co.

2.2. Synthesis of Cu-MOF/Hep

Initially, Hep (0.20 g) was dissolved in 40 mL of DMF for about 20 min to achieve a homogeneous solution. Subsequently, 0.48 g of copper (II) nitrate trihydrate (Cu $(NO_3)_2.3H_2O$, 2 mmol) was added, and the solution was stirred for 15 min. Following this, 0.32 g of terephthalic acid (2 mmol) was added, and stirring was kept for 15 min. The resulting mixture was then subjected to reflux for a duration of 24 h at a temperature of 120 °C. Finally, the reaction mixture was allowed to cool, and the resulting solid was separated by filtration, washed multiple times with DMF, and dried at room temperature (product: 0.75 ± 0.05 g) [40].

2.3. Characterization

To confirm the preparation of the catalyst, various analyses were performed. Fourier-transform Infrared spectroscopy (FT-IR) was performed using Bruker Instruments, model Aquinox 55, Germany spectrophotometer with KBr pellets. X-ray diffraction (XRD) was carried out using a Siemens, D500 with Cu-Ka radiation at 35 Kv, Japan. UV–Vis spectra were recorded using ultraviolet-visible spectroscopy (UV–Vis, Shimadzu, Model 1700, Japan). Thermo gravimetric analysis (TGA) was performed at a heating rate of 10 °C min–1 under an O_2 atmosphere (LINSEIS STA PT-1000 Germany). Scanning electron microscopy (SEM) coupled with energy-dispersive X-ray spectroscopy (EDS) was conducted using an SEM-TESCAN MIRA3-FEG, Czech Republic. Transmission Electron Microscopy (TEM Philips EM 208S instrument, Netherland) was employed for the analysis of the surface morphology of the specimens. The evaluation of Zeta potential (ZP) and dynamic light scattering (DLS) was carried out utilizing a DLS-ZP/particle sizer (Malvern model MAL1032660, England).

2.4. DOX loading

In this experiment, 50 mg of Cu-MOF/Hep was mixed with 50 mL of a solution containing 100 ppm of DOX and shaken for 48 h at room temperature in a dark tube. The resulting precipitate was centrifuged and the sample was washed with deionized water to remove any unbound drugs. The UV–vis spectroscopy method was employed to measure the quantity of DOX that was loaded onto the sample, using a calibration curve for DOX. The loading efficiency (LE) was calculated using an equation (Eq. (1)).

$$\%LE = \frac{\text{Mass of drug in nanomedicine}}{\text{Mass of drug fed initially}} \times 100 \quad (1)$$

2.5. In vitro release of DOX

The release of DOX from the nanomedicine was investigated in vitro under two different pH conditions (pH 5 and 7.4). Each nanomedicine, typically weighing 10 mg, was placed in 10 mL of PBS buffer solution in environments simulating tumor tissue (pH 5, 41 °C) and physiological conditions (pH 7.4, 37 °C). At specific time points, samples were collected from the release media and replaced with fresh medium. The UV–Vis spectrophotometer was utilized to quantify the amount of DOX released from the nanomedicine. Eq. (2) was applied to determine the percentage of DOX released.

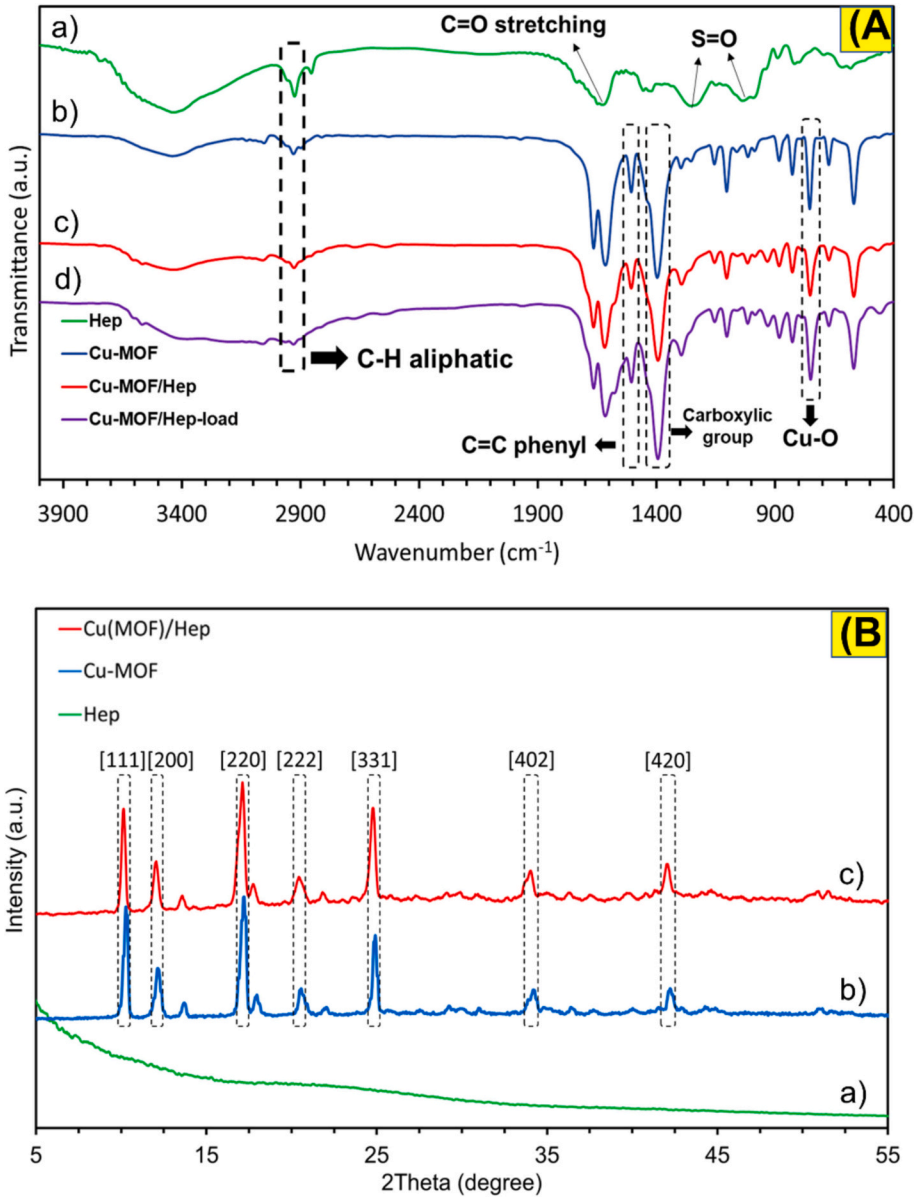

Fig. 1. (A) The FT-IR spectra of a) Hep, b) Cu-MOF, c) Cu-MOF/Hep, and d) Cu-MOF/Hep loaded with DOX. (B) The XRD pattern of a) Hep, b) Cu-MOF, and c) Cu-MOF/Hep.

$$\text{Drug release} = \frac{\text{the amount of released drug}}{\text{the amount of loaded drug}} \times 100 \quad (2)$$

2.6. Kinetics of drug release

Utilizing mathematical models including zero-order (Eq. (3)), first-order (Eq. (4)), Higuchi (Eq. (5)), Weibull (Eq. (6)), and Korsmeyer-Peppas models (Eq. (7)) for data analysis, the mechanism of DOX release from the nanomedicine was evaluated using Mathcad version 15 software [41,42]. The outcomes are documented in Table 2. In these equations, K_0, K_f, K_h, β, t_d, and F represent the drug release constant for the zero-order model, the constant for first-order drug release, Higuchi's dissolution constant, the shape parameter, the time scale of the process, and the drug release rate at a specific time t, respectively.

$$F = K_0 t \quad (3)$$

$$\text{Ln}\,(1 - F) = -K_f\, t \quad (4)$$

$$F = K_h\, t^{1/2} \quad (5)$$

$$\text{Ln}\,[-ln\,(1 - F)] = -\beta \ln t_d + \beta \ln t \quad (6)$$

$$\frac{F}{F_\infty} = K_{k\,p}\, t^n \quad (7)$$

2.7. Cytotoxicity study

MTT assays were utilized to evaluate the cytotoxicity of the synthesized materials in vitro [43]. MCF-7 cells were plated in 96-well plates at a density of 6000 cells per well in 200 μL of cell medium and incubated for 24 h. Subsequently, the cells were exposed to DOX, DOX-loaded Hep, and DOX-loaded Cu-MOF/Hep at equivalent drug concentrations. Blank Cu-MOF and Cu-MOF/Hep were also applied to test the cytocompatibility of the samples. After a 48-hour incubation period, cell viability was assessed by replacing the culture medium in each well with 50 μL of 3 mg/mL MTT solution mixed with 100 μL of fresh culture

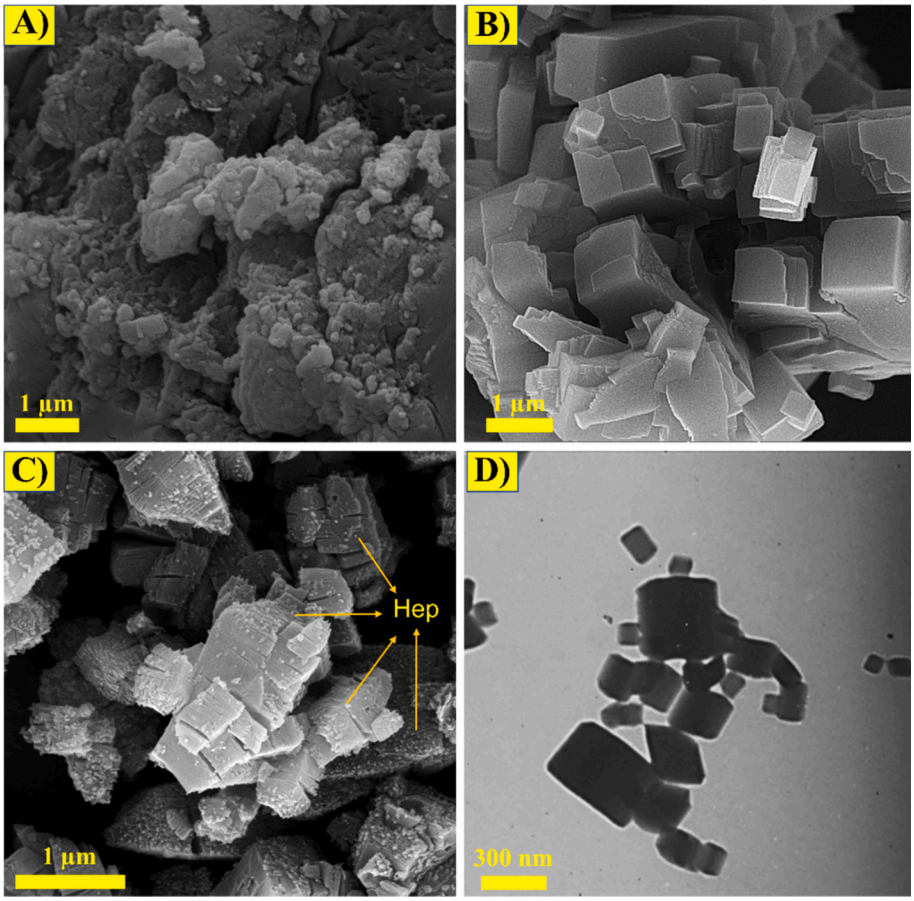

Fig. 2. The SEM and TEM image of A) Hep, B) Cu-MOF, C) Cu-MOF/Hep, and D) Cu-MOF/Hep.

medium. Following a 4-hour incubation at 37 °C, 100 µL of dimethyl sulfoxide (DMSO) was added to dissolve the formazan crystals. The cell count was determined using a hemacytometer (DANA-DA3200). Each sample was tested in triplicate to ensure the reliability of the results.

2.8. DAPI staining

DAPI staining was employed to identify nuclear condensation and fragmentation in apoptotic cells triggered by the samples (DOX, DOX/Cu-MOF/HEP, Cu-MOF/DOX). MCF-7 cells (5×10^5 cells/well) were seeded on glass coverslips and treated with samples at related IC_{50} for 48 h. Following the treatment, cells were rinsed, fixed with para-formaldehyde, permeabilized with Triton X-100, stained with DAPI, and subsequently analyzed for apoptosis using fluorescence microscopy. All procedures were conducted in triplicate.

2.9. Statistical analysis

The mean ± standard deviation was employed to present the outcomes. To determine statistical significance, a one-way analysis of variance (ANOVA) was conducted using the Microsoft Excel software, while considering a *P* value below 0.05. Each experiment was repeated a minimum of three times.

3. Result and discussion

3.1. Characterization of the nanomedicine

The FT-IR analyses were used for the characteristics of functional groups and the structure of samples. The spectrum of Cu-MOF, Hep, and Cu-MOF/Hep are shown in Fig. 1a. The peaks that appeared at 754, 1398, 1620,1506, 2922, and 3442 cm^{-1} in the Cu-MOF spectrum, are related to the stretching vibrational of the Cu—O, symmetric and asymmetric stretching of carboxylic groups, C═C bonds in phenyl rings of cross-linker, aliphatic C—H bonds, and hydroxyl groups, respectively [44,45]. In the spectrum of Hep, various peaks were presented at 1039, 1247, 1423, 1626, 2927, and 3442 cm^{-1} are associated with asymmetric and symmetric stretching of S═O bond in sulfate groups, N—H bending, C═O stretching, C—H aliphatic, and hydroxyl groups, respectively [46,47]. The spectra of Cu-MOF/Hep and its loaded composite exhibited the same peaks compared to Cu-MOF with little differences in the related C═O stretching region observed tow shoulder peaks. The differences can be attributed to the grafting Hep on the Cu-MOF structure and also the existence of a model drug (DOX) in the structure of the composite. The results confirmed the successful synthesis of Cu-MOF/Hep composites.

The powder XRD technique was employed to investigate the crystalline structure of synthesized materials. The XRD patterns of Cu-MOF, Hep, and Cu-MOF/Hep in the 2θ range of 5–55 were demonstrated in Fig. 1b. The peaks were observed at $2\theta = 10.32°$, 12.22°, 17.22°, 20.47°, 24.98°, 34.12°, and 42.22° in the Cu-MOF pattern, related to the (111), (200), (220), (222), (331), (402), and (420) planes of Cu-MOF structure, that confirmed the FCC cubic crystal structure [40,48]. In the XRD pattern of Hep, the broad peak that appeared around $2\theta = 22°$ indicates its amorphous structure [49]. The final nanocomposite spectrum (Cu-MOF/Hep) showed peaks related to Cu-MOF crystalline structure with a slight shift, possibly due to Cu-MOF functionalization with Hep. Additionally, it confirmed that the crystalline structure of the composite is preserved after functionalizing the Cu-MOF with Hep.

The SEM and TEM images of materials are shown in Fig. 2. The Hep

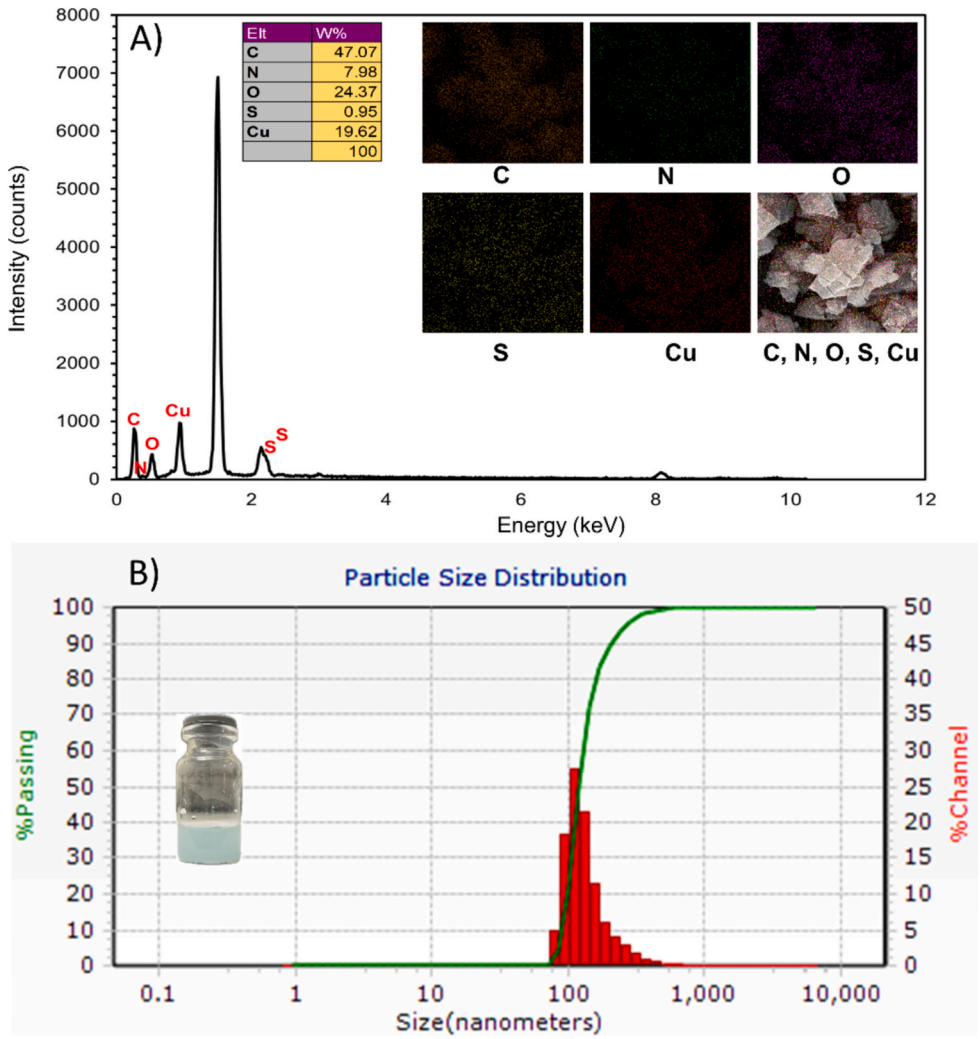

Fig. 3. The EDX and MAP analysis of Cu-MOF/Hep (A) and the particle size distribution of Cu-MOF/Hep (B) with colloidal dispersity in distilled water after 3 days.

SEM image demonstrated aggregate and amorphous structures with rough surfaces [50]. In the Cu-MOF images, the plans of the cubic structure with a smooth surface were observed which confirmed its crystalline structure [51]. The SEM image showed a cubic shape of Cu-MOF surrounded by amorphous Hep particles, indicating successful modification. Additionally, following XRD results, the TEM image of the composite presented a cubic crystal structure, which can be attributed to the Cu-MOF [52].

Moreover, the presence of C, O, N, S, and Cu within the Cu-MOF/Hep composite structure was validated through EDX analyses (Fig. 3a). Furthermore, the elemental mapping assessments revealed a uniform dispersion of these elements across the composite surface. The particle size distribution and zeta potential were utilized for measuring the particle size and surface charge in deionized water. The average particle size of the Cu-MOF/Hep concerning the diagram (Fig. 3b) was calculated to be about 100 nm. Also, Cu-MOF/Hep showed a positive charge (+29.3 mV) with PDI = 2.9 which can be related to the existence of uncoordinated metal sites (Cu^{2+}) in the structure of the MOF. This higher positive charged value can also trigger long-term colloidal dispersity for Cu-MOF/Hep even after 3 days in distilled water (inside Fig. 3b). Because of the negative charge of some cell types, such as cancer cells, there is a greater potential for interaction between positively charged Cu-MOF/Hep and these cells that can be considered as a significant feature [53].

The TGA analysis was employed to assess the thermal stability of the synthesized materials. As shown in Fig. 4, Hep demonstrated reductions in weight attributed to the loss of water as well as the hydrolysis and breakdown of Hep occurring at temperatures approximately reaching 100, 230, and 500 °C [54]. In addition, three distinct stages of weight loss were identified in Cu-MOF/Hep. The first step involves removing adsorbed water at 25–120 °C, the next stage is hydrolysis of Hep, elimination of dimethylformamide, and dehydroxylation of Cu clusters at 130–500 °C [55]. The final phase (commencing at 500 °C) is ascribed to the decomposition of Cu-MOF and Hep, resulting from the combustion of organic-linker molecules and oligomers within the Cu-MOF/Hep composite structure, demonstrating thermal resistance below 500 °C [35]. According to the third stage, the weight percentage of Hep to Cu-MOF can be calculated to be about 40 %.

3.2. *In-vitro DOX loading and release studies*

The quantity of DOX loaded in the Cu-MOF and Cu-MOF/Hep composite was estimated to be 60.2 ± 0.5 %, and 65.5 ± 0.5 %, respectively, as determined using the UV–visible spectroscopy method. This increase in the loading capacity of Cu-MOF/Hep can be related to the possible H-bonding interaction DOX molecules with Hep in addition to electrostatic π-π stacking and host-gest interactions with Cu-MOF (Scheme 1). Fig. 5 demonstrated the release profile of DOX in different pH values (i.e., 7.4 and 5) from the Cu-MOF and Cu-(MOF)/Hep. As can be seen in the release profiles, during the initial stages (24 h), the drug release from Cu-MOF demonstrates higher and faster rates in comparison to Cu-MOF/Hep. While, over time, the amount of drug released from Cu-MOF/Hep is

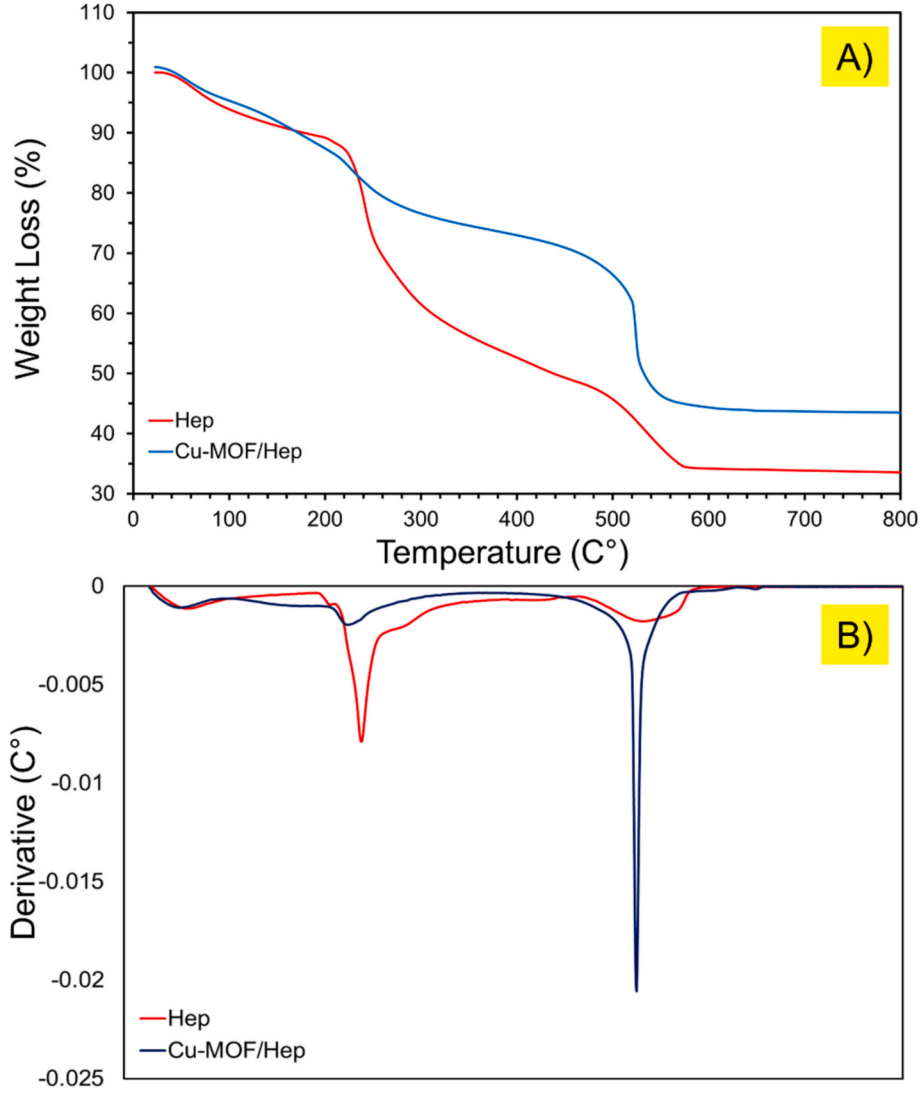

Fig. 4. The TGA (A) and DTG (B) analysis of Hep and Cu-MOF/Hep.

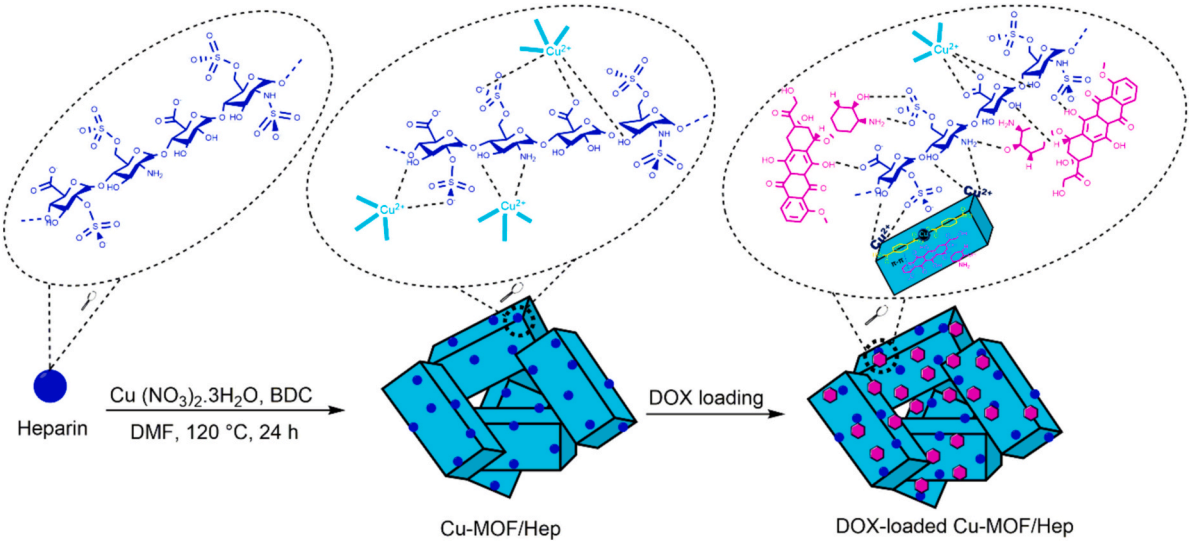

Scheme 1. Illustration of the synthesis of Cu-MOF/Hep nanomedicine.

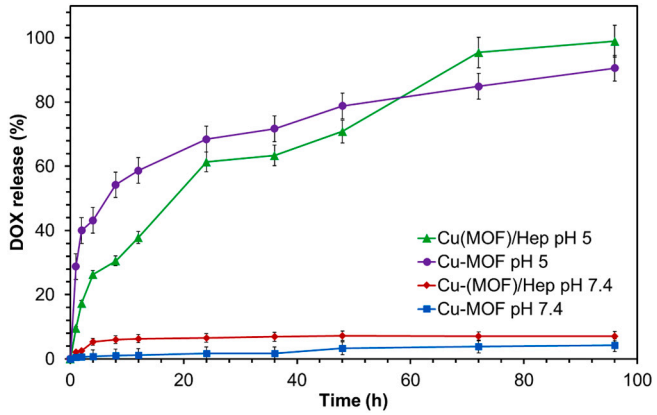

Fig. 5. The cumulative release profile of DOX from Cu-MOF and Cu-MOF/Hep at different pH (7.4, 5).

more than that of Cu-MOF. On the other hand, the release rate of the DOX from the Cu-MOF/Hep exhibited a sustained and long-term profile. On the other hand, most release of DOX from the samples occurred in acidic media (pH 5); however, the rate of released DOX from Cu-MOF/Hep was higher than Cu-MOF. This higher release percentage at pH 5 than 7.4 can be due to the sensitivity of Cu-MOF/Hep to acidic conditions, leading to the destruction of the MOF structure and releasing the loaded DOX. This can be shown by the gravimetric analysis that indicated low residual mass after treatment at pH 5 (<~35 %) than that of pH 7.4 (<~87 %) for 48 h (supporting information). Moreover, at pH 7.4, the H-bonding between the functional groups of the Heparin structure and the NH and OH groups of the DOX are stable. While, at pH 5, protonation of the DOX amino groups causes the loss of H-bonding and increases the drug's solubility and hydrophilicity [56]; therefore, DOX is rapidly released in an acidic medium. Table 1 summarizes the modified MOFs and their respective features. The drug loading and pH-sensitive release of the present Cu-MOF/Hep nanocomposite show comparable and, in some cases, improved results than that of reported previous works. Besides, the release kinetics of the DOX profile indicate that the Weibull model is the best fit for both the Cu-MOF and Cu-MOF/Hep nanocarriers (Table 2, Figs. S1 and S2). All pH conditions exhibit a single kinetic model despite the pH-sensitive nature of the release. This observation may be attributed to the dominant influence of the nanocarrier structure and the release environment, which can overshadow the effects of pH variations. Regarding the Korsmeyer-Peppas model, the release exponent (n) was calculated to better understand the release mechanisms. For this model, an exponent value of $n \leq 0.45$ suggests Fickian diffusion, while values between 0.45 and 0.89 indicate non-Fickian (anomalous) release [57]. The n value below 0.45 for all tested samples confirms that the release mechanism of the prepared nanocarriers predominantly follows Fickian diffusion (Table 2). The obtained results indicated that the Cu-MOF/Hep composite can be a suitable candidate for passive anti-cancer drug delivery [33,58].

3.3. In-vitro cytotoxicity

The cytotoxicity of the prepared nanomedicine was assessed utilizing the MTT test. The results depicted in Fig. 6 indicate that the cytotoxicity towards MCF-7 cells exhibited a dependency on both the drug dosage and incubation time. Wherein, prolonged incubation periods and high dosage of treatment resulted in higher cytotoxic effects. At the equal concentration of DOX, the cytotoxicity of the DOX-loaded Cu-MOF/Hep nanocomposite was higher than both free DOX and DOX-loaded Cu-MOF. The IC_{50} value for the DOX-loaded Cu-MOF and Cu-MOF/Hep was determined to be ~20 and 10 μg/mL after 48 h of incubation,

Table 2
The parameters of DOX release kinetics.

Kinetics models	Parameters	Cu-MOF/Hep		Cu-MOF	
		pH 5	pH 7.4	pH 5	pH 7.4
Zero-order	R^2	0.424	0.392	0.566	0.536
First-order	R^2	0.397	0.392	0.558	0.533
Higuchi	R^2	0.617	0.581	0.762	0.727
Weibull	R^2	0.999	0.953	0.984	0.967
Korsmeyer-Peppas	k_{kp}	12.182	4.866	37.321	0.196
	n	0.125	0.254	0.154	0.345
	R^2	0.975	0.935	0.901	0.946

Table 1
A summary of most applicable pH-responsive MOFs.

MOF	Modification	Drug & loading capacity (wt%)	Drug release pH = 5 pH = 7.4	Year	Ref.
CMC/TC@UiO-66	CMC hydrogel	Tetracycline (TC) 99 %	>75 % (pH 7.4)	2021	[59]
Fe_3O_4@MOF-DOX-CDs-Apt	Fluorescent carbon dots and Aptamer	Doxorubicin 60 %	>46 % <30 %	2020	[60]
CMC/MIL-88(Fe)	Carboxymethyl cellulose (CMC) fiber	Tetracycline	– >65 % over 384 h	2021	[34]
ZIF-8	–	Fluorouracil 45.4	45 % 17 %	2012	[61]
St/Fe_3O_4/MIL-88(Fe)	Magnetic starch (core)	Tetracycline 90 %	– 73 %	2023	[62]
CaZol	Dioleoylphosphatydic acid (shell)	Zoledronate 76	100 <5	2016	[63]
Fe3O4/MIL-88(Fe)	Functionalized with mannose and coated with pectin hydrogel	Methotrexate 99 %	10 % (pH 1.2) 40 % (pH 6.8) >90 % (pH 7.4)	2024	[64]
CS/GA-MOF	Chitosan (CS) hydrogel	Gentamicin Preloading (100 %)	– >65 %	2024	[65]
Fe_3O_4@UiO-66-NH_2@PEI	Schiff base reaction and polyethyleneimine (PEI)pre-adsorption	Imatinib 94 %	<40 % >90 %	2023	[66]
ZnO-DOX@ZIF-8	ZnO (core)	Doxorubicin 11.2	80 % (pH 5.5) 20 %	2017	[67]
ZIF-8@PAAS	Poly(acrylic acid sodium salt)	Doxorubicin 173–385	>60 % <15 %	2017	[68]
Cu-MOF/Hep	In-situ Hep functionalization	Doxorubicin 65 %	>90 % <5 %	–	This work

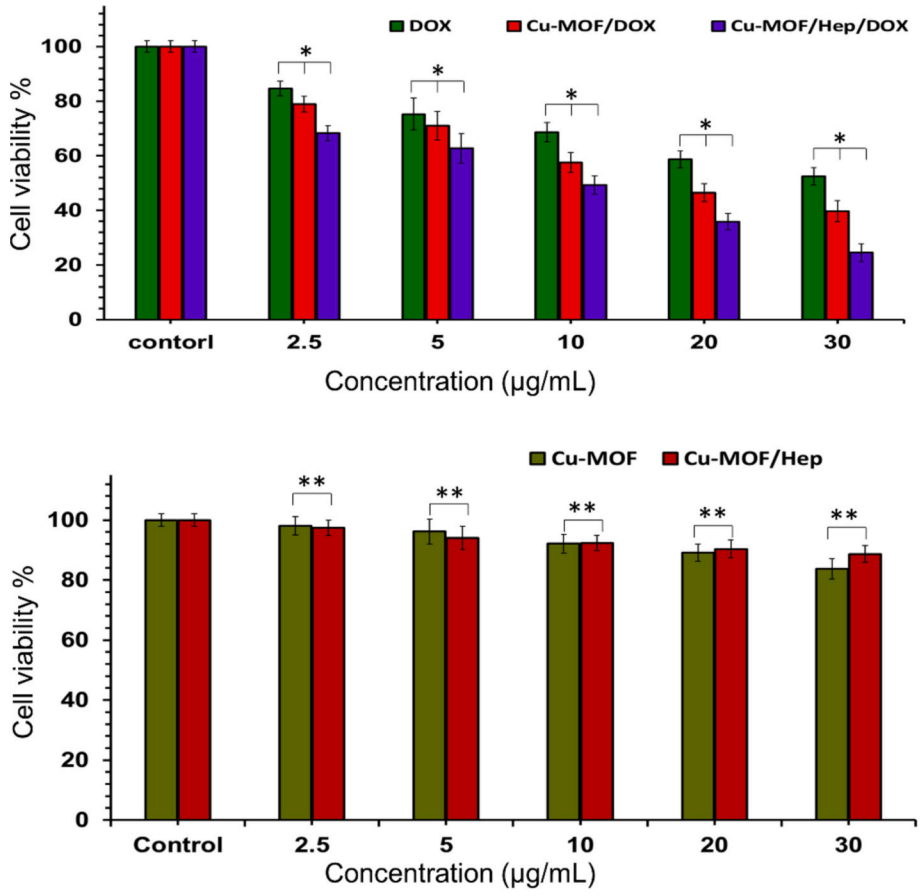

Fig. 6. The result of MTT analysis against MCF-7 cells after 48 h incubation at different concentrations of DOX, DOX-loaded Cu-MOF, and Cu-MOF/Hep (*$P < 0.05$, **$P < 0.05$).

respectively. The increased cytotoxicity observed in the DOX-loaded Cu-MOF/Hep nanocomposite can be attributed to several factors. Firstly, the positively charged nature of the nanomedicine enhances its interaction with negatively charged cellular components, such as nucleic acids, thereby facilitating improved cellular uptake [69–71]. Additionally, the presence of amide bonds within the Hep structure may further enhance this interaction, promoting a more effective binding to cells and tissues upon entry. This mechanism is particularly relevant in the context of cancer treatment, where the ability of nanoparticles to accumulate in tumor sites is crucial. The enhanced permeability and retention (EPR) effect plays a significant role in the therapeutic efficacy of heparin-modified systems [72]. The leaky and discontinuous blood vessels found in tumor tissues, resulting from rapid angiogenesis, allow for the accumulation of nanoparticles within the tumor microenvironment. The size of the Cu-MOF/Hep nanocomposite (about 100 nm) can facilitate this extravasation, while normal vessels exhibit limited permeability [73]. The blank nanomedicine exhibited good cytocompatibility characteristics and cell viability remained over 90 %

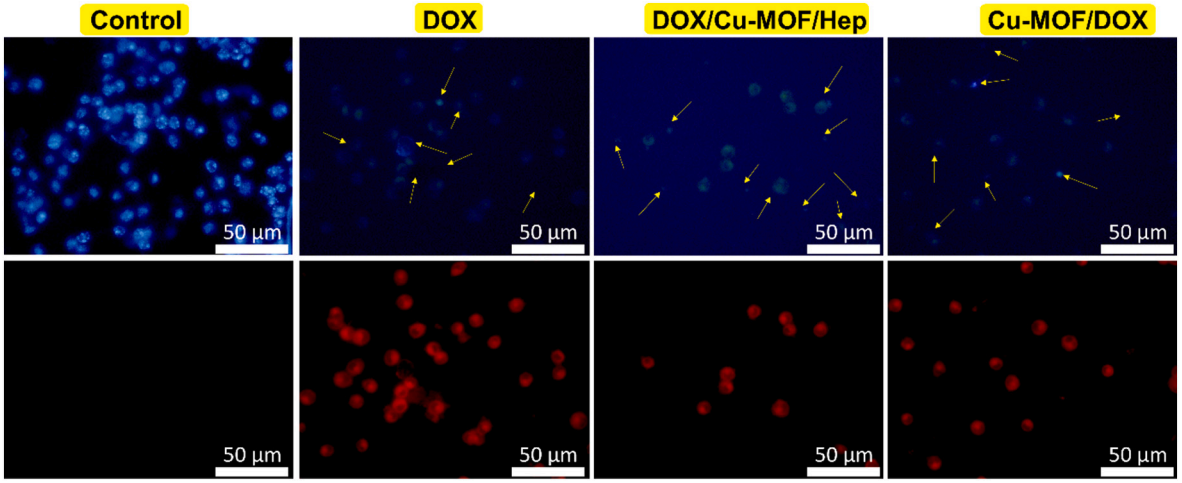

Fig. 7. Apoptosis study by DAPI staining after treatment of MCF-7 with DOX, DOX/Cu-MOF/Hep, and Cu-MOF/DOX for 24 h at 37 °C (above images stand for blue channel and below images stand for red channel).

following a 48-h incubation period even at 7 μg/mL concentration. A similar result was explained by Safarkhani et al. [74], describing MOF-based nanocomposite has good cytocompatibility against cancerous cells. Based on the findings, the Cu-MOF/Hep nanomedicine could potentially serve as a promising platform for anticancer DDSs.

3.4. Cellular apoptosis studies

For the analysis of apoptotic characteristics, DAPI staining, a reliable technique for identifying cell apoptosis and necrosis based on its ability to bind to cell nuclei, was utilized in conjunction with fluorescence imaging. In this study, MCF-7 cells were exposed to DOX, DOX-loaded Cu-MOF, and Cu-MOF/Hep, and their structural features were assessed (as illustrated in Fig. 7). Cells treated with DOX-loaded Cu-MOF/Hep exhibited a significant decrease in viability compared with control, accompanied by enhanced blue fluorescence indicating nuclei fragmentation and chromatin condensation (displayed with arose and sings in Fig. 7). The ratio of apoptosis cells was determined to be about 18, 42, 63 % and for DOX, DOX/Cu-MOF and DOX/Cu-MOF/Hep, respectively. The use of active targeting nanomedicine for delivering anticancer drugs shows promise in overcoming multidrug resistance (MDR) [71,75]. Receptor-targeted nanocarriers offer a novel approach to combat MDR by facilitating targeted endocytosis in cancer cells. As shown in fluorescence images related to DOX excitation (Fig. 7), the apoptosis was notably enhanced when using DOX-loaded Cu-MOF/Hep. This implies that DOX can be transported into cancer cells through the Hep-functionalized nanomedicine, potentially evading MDR-associated efflux, commonly referred to as “stealth” endocytosis. Additionally, the presence of Hep in the Cu-MOF/Hep architecture facilitated apoptosis initiation and cancer cell targeting via the CD44 receptor while preserving the integrity of DOX [32,76]. These results align with those of the MTT and cellular apoptosis analyses, supporting the successful internalization of Cu-MOF/Hep by cells. In conclusion, these outcomes suggest that Cu-MOF/Hep shows promise as an active targeting drug nanocarrier for enhancing cancer therapy.

4. Conclusion

Briefly, the nanomedicine was synthesized by a one-pot synthesis method. Then various analytical techniques were employed to characterize and confirm the synthesized nanocomposite, including XRD, SEM, FT-IR, TEM, DLS, TGA, and ZP. The innovative combination of Cu-based MOFs with saccharides like Hep in the creation of a targeting drug delivery system, Cu-MOF/Hep, showed controlled release profiles and improved drug efficacy. In vitro DOX release studies revealed higher release rates (>90 % after 96 h) under conditions simulating tumor tissue (pH 5, 41 °C) compared to standard physiological conditions (pH 7.4, 37 °C, <20 % after 96 h), as well as notable cytotoxic effects of DOX-loaded Cu-MOF/Hep on MCF-7 cells (IC_{50}: ~10 μg/mL). The integration of MOF structures modified with receptors in DDSs represents a promising approach to enhancing the efficacy and safety of cancer therapy. Overall, the findings suggest that the Cu-MOF/Hep nanocomposite has the potential to be a promising platform for active and passive targeting delivery of anticancer agents with enhanced effectiveness and safety.

The promising in vitro results, including controlled release rates of DOX and significant cytotoxic effects on cancer cells, indicate a strong potential for clinical application. However, transitioning to clinical stages will require further studies, including in vivo testing to assess safety, efficacy, and pharmacokinetics. The use of Cu-based materials raises concerns regarding in vivo toxicity, which must be thoroughly investigated. Additionally, understanding the biodistribution of the Cu-MOF/Hep system in the body and its blood circulation time is crucial for evaluating its safety and efficacy. These factors will significantly influence the clinical applicability of the nanocomposite and should be included in future studies to provide a comprehensive assessment of its potential as a therapeutic agent. However, according to the obtained results, the present study confirms the favorable outcomes observed in vitro; therefore, the Cu-MOF/Hep system could be a viable candidate for clinical trials in cancer therapy. Looking ahead, we propose that future studies could explore the structural comparisons between Hep analogs and other compounds (i.e., folic acid, hyaluronic acid, anisamide, etc.) that can enhance the efficacy of DOX. Specifically, the incorporation of phytochemicals or other synergistic agents (naturally found phenolic compounds: such as taxol analogs and vinca alkaloids) into the Cu-MOF-Hep configuration could potentially improve therapeutic outcomes. These ingredients may work in concert with the existing components to enhance drug delivery and efficacy, opening new avenues for research in targeted cancer therapy.

CRediT authorship contribution statement

Sima Darvishi: Writing – original draft, Visualization, Software, Methodology, Investigation, Formal analysis, Conceptualization. **Hossein Hosseinzadeh:** Writing – original draft, Investigation, Formal analysis. **Fahimeh Kazeminava:** Validation, Investigation, Formal analysis. **Amin Mahoutforoush:** Investigation, Formal analysis. **Mohammadreza Tajik:** Investigation, Formal analysis. **Monireh Rasoulzadehzali:** Formal analysis. **Reza Mohammadi:** Writing – review & editing, Validation, Supervision, Resources. **Samaheh Sadjadi:** Writing – review & editing, Validation, Supervision, Resources. **Siamak Javanbakht:** Writing – review & editing, Validation, Supervision, Resources, Project administration.

Declaration of competing interest

The authors declare that they have no known competing financial interests or personal relationships that could have appeared to influence the work reported in this paper.

Acknowledgments

This research is supported by the research grant of the University of Tabriz (number SAD/2389-14020820).

Appendix A. Supplementary data

Supplementary data to this article can be found online at https://doi.org/10.1016/j.ijbiomac.2024.136648.

Data availability

The data that support the findings of this study are available from the corresponding author, upon reasonable request.

References

[1] J. Liu, A. Zangeneh, M.M. Zangeneh, B. Guo, Antioxidant, cytotoxicity, anti-human esophageal squamous cell carcinoma, anti-human Caucasian esophageal carcinoma, anti-adenocarcinoma of the gastroesophageal junction, and anti-distal esophageal adenocarcinoma properties of gold nanoparticles green synthesized by *Rhus coriaria* L. fruit aqueous extract, J. Exp. Nanosci. 15 (1) (2020) 202–216, https://doi.org/10.1080/17458080.2020.1766675.

[2] T.N. Seyfried, L.M. Shelton, Cancer as a metabolic disease, Ann. Nutr. Metab. 7 (2010) 1–22, https://doi.org/10.1186/1743-7075-7-7.

[3] L. Ma, A. Ahmeda, K. Wang, A.R. Jalalvand, K. Sadrjavadi, M. Nowrozi, A. Zangeneh, M.M. Zangeneh, X. Wang, Introducing a novel chemotherapeutic drug formulated by iron nanoparticles for the clinical trial studies, Appl. Organomet. Chem. 36 (12) (2022) e5498, https://doi.org/10.1002/aoc.5498.

[4] Y. Li, N. Li, W. Jiang, G. Ma, M.M. Zangeneh, In situ decorated Au NPs on pectin-modified Fe_3O_4 NPs as a novel magnetic nanocomposite (Fe_3O_4/Pectin/Au) for catalytic reduction of nitroarenes and investigation of its anti-human lung cancer activities, Int. J. Biol. Macromol. 163 (2020) 2162–2171, https://doi.org/10.1016/j.ijbiomac.2020.09.102.

[5] A. Dehnoee, R. Javad Kalbasi, M.M. Zangeneh, M.R. Delnavazi, A. Zangeneh, One-step synthesis of silver nanostructures using *Heracleum persicum* fruit extract, their cytotoxic activity, anti-cancer and anti-oxidant activities, Micro Nano Lett. 18 (1) (2023) e12153, https://doi.org/10.1049/mna2.12153.

[6] M. Hassan, J. Ansari, D. Spooner, S. Hussain, Chemotherapy for breast cancer, Oncol. Rep. 24 (5) (2010) 1121–1131.

[7] D.T. Debela, S.G. Muzazu, K.D. Heraro, M.T. Ndalama, B.W. Mesele, D.C. Haile, S. K. Kitui, T. Manyazewal, New approaches and procedures for cancer treatment: current perspectives, SAGE Open Med. 9 (2021) 20503121211034366, https://doi.org/10.1177/20503121211034366.

[8] G. Manish, S. Vimukta, Targeted drug delivery system: a review, Res. J. Chem. Sci. 1 (2) (2011) 135–138.

[9] V. Jain, S. Jain, S. Mahajan, Nanomedicines based drug delivery systems for anti-cancer targeting and treatment, Curr. Drug Deliv. 12 (2) (2015) 177–191.

[10] J. Bai, X. Gongsun, L. Xue, M.M. Zangeneh, Introducing a modern chemotherapeutic drug formulated by iron nanoparticles for the treatment of human lung cancer, J. Exp. Nanosci. 16 (1) (2021) 397–409, https://doi.org/10.1080/17458080.2021.1998460.

[11] A. Ahmeda, A. Zangeneh, M.M. Zangeneh, Green synthesis and chemical characterization of gold nanoparticle synthesized using *Camellia sinensis* leaf aqueous extract for the treatment of acute myeloid leukemia in comparison to daunorubicin in a leukemic mouse model, Appl. Organomet. Chem. 34 (3) (2020) e5290, https://doi.org/10.1002/aoc.5290.

[12] F. Oroojalian, S. Karimzadeh, S. Javanbakht, M. Hejazi, B. Baradaran, T.J. Webster, A. Mokhtarzadeh, R.S. Varma, P. Kesharwani, A. Sahebkar, Current trends in stimuli-responsive nanotheranostics based on metal–organic frameworks for cancer therapy, Mater. Today 57 (2022) 192–224, https://doi.org/10.1016/j.mattod.2022.05.024.

[13] S. Kitagawa, Metal–organic frameworks (MOFs), Chem. Soc. Rev. 43 (16) (2014) 5415–5418, https://doi.org/10.1039/C4CS90059F.

[14] H.-C. Zhou, Jeffrey R. Long, Omar M. Yaghi, Introduction to metal–organic frameworks, Chem. Rev. 112 (2) (2012) 673–674, https://doi.org/10.1021/cr300014x.

[15] M. Giménez-Marqués, T. Hidalgo, C. Serre, P. Horcajada, Nanostructured metal–organic frameworks and their bio-related applications, Chem. Rev. 307 (2016) 342–360, https://doi.org/10.1016/j.ccr.2015.08.008.

[16] B.A. Lakshmi, S. Kim, Current and emerging applications of nanostructured metal–organic frameworks in cancer-targeted theranostics, Mater. Sci. Eng. C 105 (2019) 110091, https://doi.org/10.1016/j.msec.2019.110091.

[17] B. Kateb, K. Chiu, K.L. Black, V. Yamamoto, B. Khalsa, J.Y. Ljubimova, H. Ding, R. Patil, J.A. Portilla-Arias, M. Modo, Nanoplatforms for constructing new approaches to cancer treatment, imaging, and drug delivery: what should be the policy? Neuroimage 54 (2011) S106–S124, https://doi.org/10.1016/j.neuroimage.2010.01.105.

[18] S. Masrour, A. Motavalizadehkakhky, M. Hosseiny, J. Mehrzad, R. Zhiani, F. Kazeminava, Soy protein isolate-based hybrid electrospun nanofibers: an enhanced antimicrobial bio-platform for potential wound healing, J. Environ. Polym. Degrad. 31 (8) (2023) 3433–3444, https://doi.org/10.1007/s10924-023-02812-2.

[19] C. Hao, H. Xu, L. Yu, L. Zhang, Heparin: an essential drug for modern medicine, PMBTS 163 (2019) 1–19, https://doi.org/10.1016/bs.pmbts.2019.02.002.

[20] M.M. Kemp, R.J. Linhardt, Heparin-based nanoparticles, Wiley Interdiscip. Rev.: Nanomed. Nanobiotechnol. 2 (1) (2010) 77–87, https://doi.org/10.1002/wnan.68.

[21] V.M. Thanh, T.H. Nguyen, T.V. Tran, U.-T.P. Ngoc, M.N. Ho, T.T. Nguyen, Y.N. T. Chau, N.Q. Tran, C.K. Nguyen, D.H. Nguyen, Low systemic toxicity nanocarriers fabricated from heparin-mPEG and PAMAM dendrimers for controlled drug release, Mater. Sci. Eng. C 82 (2018) 291–298, https://doi.org/10.1016/j.jcou.2016.04.008.

[22] Y. Liang, K.L. Kiick, Heparin-functionalized polymeric biomaterials in tissue engineering and drug delivery applications, Acta Biomater. 10 (4) (2014) 1588–1600, https://doi.org/10.1016/j.actbio.2013.07.031.

[23] J. Yang, X. Meng, Y. Rao, X. Wang, S. Meng, C. Teng, T. Sun, C. Zong, Harnessing the potential of de-sulfated heparin for targeted drug delivery: a three-component approach exemplified by conjugation with galactose and paclitaxel, Carbohydr. Polym. (2024) 121986, https://doi.org/10.1016/j.carbpol.2024.121986.

[24] J. Heino, J. Kapyla, Cellular receptors of extracellular matrix molecules, Curr. Pharm. Des. 15 (12) (2009) 1309–1317, https://doi.org/10.2174/138161209787846720.

[25] U. Jarouliya, R.K. Keservani, Protein function as cell surface and nuclear receptor in human diseases, in: Medicinal Chemistry with Pharmaceutical Product Development, Apple Academic Press, 2019, pp. 1–32.

[26] S. Misra, V.C. Hascall, R.R. Markwald, S. Ghatak, Interactions between hyaluronan and its receptors (CD44, RHAMM) regulate the activities of inflammation and cancer, Front. Immunol. 6 (2015) 201, https://doi.org/10.3389/fimmu.2015.00201.

[27] I. Capila, R.J. Linhardt, Heparin–protein interactions, Angew. Chem. Int. Ed. Engl. 41 (3) (2002) 390–412, https://doi.org/10.1002/1521-3773(20020201)41:3%3C390::AID-ANIE390%3E3.0.CO;2-B.

[28] R. van der Voort, T.E. Taher, V.J. Wielenga, M. Spaargaren, R. Prevo, L. Smit, G. David, G. Hartmann, E. Gherardi, S.T. Pals, Heparan sulfate-modified CD44 promotes hepatocyte growth factor/scatter factor-induced signal transduction through the receptor tyrosine kinase c-Met, JBC 274 (10) (1999) 6499–6506, https://doi.org/10.1074/jbc.274.10.6499.

[29] D. Shukla, J. Liu, P. Blaiklock, N.W. Shworak, X. Bai, J.D. Esko, G.H. Cohen, R. J. Eisenberg, R.D. Rosenberg, P.G. Spear, A novel role for 3-O-sulfated heparan sulfate in herpes simplex virus 1 entry, Cell 99 (1) (1999) 13–22, https://doi.org/10.1016/S0092-8674(00)80058-6.

[30] M.H. Akhter, M. Rizwanullah, J. Ahmad, M.J. Ahsan, M.A. Mujtaba, S. Amin, Nanocarriers in advanced drug targeting: setting novel paradigm in cancer therapeutics, Artif. Cells Nanomed. Biotechnol. 46 (5) (2018) 873–884, https://doi.org/10.1080/21691401.2017.1366333.

[31] M. Habban Akhter, S. Amin, An investigative approach to treatment modalities for squamous cell carcinoma of skin, Curr. Drug Deliv. 14 (5) (2017) 597–612, https://doi.org/10.2174/1567201801666160906104254.

[32] X. Sun, Y. Li, L. Xu, X. Shi, M. Xu, X. Tao, G. Yang, Heparin coated meta-organic framework co-delivering doxorubicin and quercetin for effective chemotherapy of lung carcinoma, Int. J. Med. Res. 48 (2) (2020) 0300060519897185, https://doi.org/10.1177/0300060519897185.

[33] H. Poursadegh, V. Bakhshi, M.S. Amini-Fazl, Z. Adibag, F. Kazeminava, S. Javanbakht, Incorporating mannose-functionalized hydroxyapatite/metal-organic framework into the hyaluronic acid hydrogel film: a potential dual-targeted oral anticancer delivery system, Int. J. Biol. Macromol. (2024) 133516, https://doi.org/10.1016/j.ijbiomac.2024.133516.

[34] S. Darvishi, S. Javanbakht, A. Heydari, F. Kazeminava, P. Gholizadeh, M. Mahdipour, A. Shaabani, Ultrasound-assisted synthesis of MIL-88 (Fe) coordinated to carboxymethyl cellulose fibers: a safe carrier for highly sustained release of tetracycline, Int. J. Biol. Macromol. 181 (2021) 937–944, https://doi.org/10.1016/j.ijbiomac.2021.04.092.

[35] S. Javanbakht, R. Mohammadian, H. Farhid, A. Shaabani, M.M. Amini, A green, reusable and remarkable catalyst for selective aerobic oxidation of alcohols: construction of Cu (BDC) on the surface of carboxymethyl cellulose fiber, Mater. Today Commun. 28 (2021) 102502, https://doi.org/10.1016/j.mtcomm.2021.102502.

[36] S. Darvishi, S. Sadjadi, E. Monflier, A. Heydari, M.M. Heravi, Sulfonic acid-functionalized k-carrageenan/Cr-based metal-organic framework: an efficient and recyclable catalyst for fructose conversion to 5-hydroxymethylfurfural, Int. J. Biol. Macromol. 264 (2024) 130555, https://doi.org/10.1016/j.ijbiomac.2024.130555.

[37] S. Javanbakht, P. Nezhad-Mokhtari, A. Shaabani, N. Arsalani, M. Ghorbani, Incorporating Cu-based metal-organic framework/drug nanohybrids into gelatin microsphere for ibuprofen oral delivery, Mater. Sci. Eng. C 96 (2019) 302–309, https://doi.org/10.1016/j.msec.2018.11.028.

[38] J.-E. Cun, X. Fan, Q. Pan, W. Gao, K. Luo, B. He, Y. Pu, Copper-based metal–organic frameworks for biomedical applications, Adv. Colloid Interf. Sci. (2022) 102686, https://doi.org/10.1016/j.cis.2022.102686.

[39] M. Abbasian, M. Khayyatalimohammadi, In-situ forming Cu-based metal-organic framework in the presence of chitosan-Fe_3O_4 nanohybrids: a pH-sensitive carrier for controlled release of doxorubicin, Int. J. Biol. Macromol. 278 (2024) 134224, https://doi.org/10.1016/j.ijbiomac.2024.134224.

[40] S. Javanbakht, M. Pooresmaeil, H. Hashemi, H. Namazi, Carboxymethylcellulose capsulated Cu-based metal-organic framework-drug nanohybrid as a pH-sensitive nanocomposite for ibuprofen oral delivery, Int. J. Biol. Macromol. 119 (2018) 588–596, https://doi.org/10.1016/j.ijbiomac.2018.07.181.

[41] S. Javanbakht, A. Hemmati, H. Namazi, A. Heydari, Carboxymethylcellulose-coated 5-fluorouracil@ MOF-5 nano-hybrid as a bio-nanocomposite carrier for the anticancer oral delivery, Int. J. Biol. Macromol. 155 (2020) 876–882, https://doi.org/10.1016/j.ijbiomac.2019.12.007.

[42] C. Luo, Q. Yang, X. Lin, C. Qi, G. Li, Preparation and drug release property of tanshinone IIA loaded chitosan-montmorillonite microspheres, Int. J. Biol. Macromol. 125 (2019) 721–729, https://doi.org/10.1016/j.ijbiomac.2018.12.072.

[43] H. Yang, D.H. Bremner, L. Tao, H. Li, J. Hu, L. Zhu, Carboxymethyl chitosan-mediated synthesis of hyaluronic acid-targeted graphene oxide for cancer drug delivery, Carbohydr. Polym. 135 (2016) 72–78, https://doi.org/10.1016/j.carbpol.2015.08.058.

[44] N.E. Tari, A. Tadjarodi, J. Tamnanloo, S. Fatemi, Synthesis and property modification of MCM-41 composited with Cu (BDC) MOF for improvement of CO_2 adsorption Selectivity, J. CO_2 Util. 14 (2016) 126–134, https://doi.org/10.1016/j.jcou.2016.04.008.

[45] G. Wang, A. Ahmeda, Z. Malek, S. Mansooridara, A. Zangeneh, M.M. Zangeneh, Chemical characterization and therapeutic properties of *Achillea biebersteinii* leaf aqueous extract synthesized copper nanoparticles against methamphetamine-induced cell death in PC12: a study in the nanotechnology and neurology fields, Appl. Organomet. Chem. 34 (4) (2020) e5488, https://doi.org/10.1002/aoc.5488.

[46] N. Bogdan, E.M. Rodríguez, F. Sanz-Rodríguez, M.C.I. de la Cruz, Á. Juarranz, D. Jaque, J.G. Solé, J.A. Capobianco, Bio-functionalization of ligand-free upconverting lanthanide doped nanoparticles for bio-imaging and cell targeting, Nanoscale 4 (12) (2012) 3647–3650, https://doi.org/10.1039/C2NR30982C.

[47] H. Zhao, H. Su, A. Ahmeda, Y. Sun, Z. Li, M.M. Zangeneh, M. Nowrozi, A. Zangeneh, R. Moradi, Biosynthesis of copper nanoparticles using *Allium eriophyllum* Boiss leaf aqueous extract; characterization and analysis of their antimicrobial and cutaneous wound-healing potentials, Appl. Organomet. Chem. 36 (12) (2022) e5587, https://doi.org/10.1002/aoc.5587.

[48] C.G. Carson, K. Hardcastle, J. Schwartz, X. Liu, C. Hoffmann, R.A. Gerhardt, R. Tannenbaum, Synthesis and structure characterization of copper terephthalate metal–organic frameworks, Wiley Online Library (2009), https://doi.org/10.1002/ejic.200801224.

[49] R. Harris, E. Lecumberri, A. Heras, Chitosan-genipin microspheres for the controlled release of drugs: clarithromycin, tramadol and heparin, Mar. Drugs 8 (6) (2010) 1750–1762, https://doi.org/10.3390/md8061750.

[50] Y.-L. Lai, C.-R. Lin, C.-C. Yen, S.-K. Yen, Heparin-loaded composite coatings on porous stent from pure magnesium for biomedical applications, J. Funct. Biomater. 14 (10) (2023) 519, https://doi.org/10.3390/jfb14100519.

[51] B. Abdollahi, S. Farshnama, E.A. Asl, A. Najafidoust, M. Sarani, Cu (BDC) metal–organic framework (MOF)-based Ag_2CrO_4 heterostructure with enhanced solar-light degradation of organic dyes, Inorg. Chem. Commun. 138 (2022) 109236, https://doi.org/10.1016/j.inoche.2022.109236.

[52] R.S. Salama, S. El-Hakam, S. Samra, S. El-Dafrawy, A. Ahmed, Adsorption, equilibrium and kinetic studies on the removal of methyl orange dye from aqueous solution by using of copper metal organic framework (Cu-BDC), Int. J. Modern Chem. 10 (2) (2018) 195–207.
[53] S. Javanbakht, M. Pooresmaeil, H. Namazi, Green one-pot synthesis of carboxymethylcellulose/Zn-based metal-organic framework/graphene oxide bio-nanocomposite as a nanocarrier for drug delivery system, Carbohydr. Polym. 208 (2019) 294–301, https://doi.org/10.1016/j.carbpol.2018.12.066.
[54] M.M. Sk, C.Y. Yue, R.K. Jena, Facile growth of heparin-controlled porous polyaniline nanofiber networks and their application in supercapacitors, RSC Adv. 4 (10) (2014) 5188–5197, https://doi.org/10.1039/C3RA45774E.
[55] Q. Yang, H.-Y. Zhang, L. Wang, Y. Zhang, J. Zhao, Ru/UiO-66 catalyst for the reduction of nitroarenes and tandem reaction of alcohol oxidation/Knoevenagel condensation, ACS Omega 3 (4) (2018) 4199–4212, https://doi.org/10.1021/acsomega.8b00157.
[56] S. Javanbakht, A. Saboury, A. Shaabani, R. Mohammadi, M. Ghorbani, Doxorubicin imprinted photoluminescent polymer as a pH-responsive nanocarrier, ACS Appl. Bio Mater. 3 (7) (2020) 4168–4178, https://doi.org/10.1021/acsabm.0c00254.
[57] R.V. Contri, R.P. Gazzi, A.R. Pohlmann, S.S. Guterres, L.A. Frank, Drug release from pharmaceutical nanocarriers, in: The ADME Encyclopedia: A Comprehensive Guide on Biopharmacy and Pharmacokinetics, Springer, 2022, pp. 419–428.
[58] A. Mohammadzadeh, S. Javanbakht, R. Mohammadi, Magnetic alginate core-shell nanoparticles based on Schiff-base imine bonding for pH-responsive doxorubicin delivery system, Colloids Surf. A: Physicochem. Eng. (2024) 134473, https://doi.org/10.1016/j.colsurfa.2024.134473.
[59] S. Javanbakht, M. Nabi, M. Shadi, M.M. Amini, A. Shaabani, Carboxymethyl cellulose/tetracycline@ UiO-66 nanocomposite hydrogel films as a potential antibacterial wound dressing, Int. J. Biol. Macromol. 188 (2021) 811–819, https://doi.org/10.1016/j.ijbiomac.2021.08.061.
[60] H. Alijani, A. Noori, N. Faridi, S.Z. Bathaie, M.F. Mousavi, Aptamer-functionalized Fe_3O_4@ MOF nanocarrier for targeted drug delivery and fluorescence imaging of the triple-negative MDA-MB-231 breast cancer cells, J. Solid State Chem. 292 (2020) 121680, https://doi.org/10.1016/j.jssc.2020.121680.
[61] C.-Y. Sun, C. Qin, X.-L. Wang, G.-S. Yang, K.-Z. Shao, Y.-Q. Lan, Z.-M. Su, P. Huang, C.-G. Wang, E.-B. Wang, Zeolitic imidazolate framework-8 as efficient pH-sensitive drug delivery vehicle, Dalton Trans. 41 (23) (2012) 6906–6909, https://doi.org/10.1039/C2DT30357D.
[62] M. Abbasian, M. Khayyatalimohammadi, Ultrasound-assisted synthesis of MIL-88 (Fe) conjugated starch-Fe_3O_4 nanocomposite: a safe antibacterial carrier for controlled release of tetracycline, Int. J. Biol. Macromol. 234 (2023) 123665, https://doi.org/10.1016/j.ijbiomac.2023.123665.
[63] K.M. Au, A. Satterlee, Y. Min, X. Tian, Y.S. Kim, J.M. Caster, L. Zhang, T. Zhang, L. Huang, A.Z. Wang, Folate-targeted pH-responsive calcium zoledronate nanoscale metal-organic frameworks: turning a bone antiresorptive agent into an anticancer therapeutic, Biomaterials 82 (2016) 178–193, https://doi.org/10.1016/j.biomaterials.2015.12.018.
[64] H. Poursadegh, M.S. Amini-Fazl, S. Javanbakht, F. Kazeminava, Magnetic nanocomposite through coating mannose-functionalized metal-organic framework with biopolymeric pectin hydrogel beads: a potential targeted anticancer oral delivery system, Int. J. Biol. Macromol. 254 (2024) 127702, https://doi.org/10.1016/j.ijbiomac.2023.127702.
[65] H. Hamedi, S. Javanbakht, R. Mohammadi, In-situ synthesis of copper-gallic acid metal–organic framework into the gentamicin-loaded chitosan hydrogel bead: a synergistic enhancement of antibacterial properties, J. Ind. Eng. Chem. 133 (2024) 454–463, https://doi.org/10.1016/j.jiec.2023.12.021.
[66] R. Shahin, M. Yousefi, H. Ziyadi, M. Bikhof, M. Hekmati, pH-Responsive and magnetic Fe_3O_4@ UiO-66-NH2@ PEI nanocomposite as drug nanocarrier: loading and release study of Imatinib, Inorg. Chem. Commun. 147 (2023) 110186, https://doi.org/10.1016/j.inoche.2022.110186.
[67] C. Zheng, Y. Wang, S.Z.F. Phua, W.Q. Lim, Y. Zhao, ZnO–DOX@ ZIF-8 core–shell nanoparticles for pH-responsive drug delivery, ACS Biomater. Sci. Eng. 3 (10) (2017) 2223–2229, https://doi.org/10.1021/acsbiomaterials.7b00435.
[68] L. Yan, X. Chen, Z. Wang, X. Zhang, X. Zhu, M. Zhou, W. Chen, L. Huang, V.A. Roy, P.K. Yu, Size controllable and surface tunable zeolitic imidazolate framework-8–poly (acrylic acid sodium salt) nanocomposites for pH responsive drug release and enhanced in vivo cancer treatment, ACS Appl. Mater. Interfaces 9 (38) (2017) 32990–33000, https://doi.org/10.1021/acsami.7b10064.
[69] A. Saboury, R. Mohammadi, S. Javanbakht, M. Ghorbani, Doxorubicin imprinted magnetic polymethacrylamide as a pH-sensitive anticancer nanocarrier, J. Drug Deliv. Technol. 79 (2023) 103998, https://doi.org/10.1016/j.jddst.2022.103998.
[70] A. Shaabani, R. Afshari, Synthesis of carboxamide-functionalized multiwall carbon nanotubes via Ugi multicomponent reaction: water-dispersible peptidomimetic nanohybrid as controlled drug delivery vehicle, ChemistrySelect 2 (18) (2017) 5218–5225, https://doi.org/10.1002/slct.201700615.
[71] Z. Chen, T. Shi, L. Zhang, P. Zhu, M. Deng, C. Huang, T. Hu, L. Jiang, J. Li, Mammalian drug efflux transporters of the ATP binding cassette (ABC) family in multidrug resistance: a review of the past decade, Cancer Lett. 370 (1) (2016) 153–164, https://doi.org/10.1016/j.addr.2012.09.027.
[72] X. Yang, H. Du, J. Liu, G. Zhai, Advanced nanocarriers based on heparin and its derivatives for cancer management, Biomacromolecules 16 (2) (2015) 423–436, https://doi.org/10.1021/bm501532e.
[73] X. Pan, P. Li, L. Bai, J. Ma, S. Li, F. Zhang, S. Liu, Q. Wu, H. Shen, H. Liu, Biodegradable nanocomposite with dual cell-tissue penetration for deep tumor chemo-phototherapy, Small 16 (22) (2020) 2000809, https://doi.org/10.1002/smll.202000809.
[74] M. Safarkhani, A. Ojaghi, S.M. Nezhad, H. Daneshgar, A.C. Paiva-Santos, F. Radmanesh, M. Bagherzadeh, E.N. Zare, N. Rabiee, P. Makvandi, Engineered (NH2)-MIL-125 (Ti)/copolymer@ $MnFe_2O_4$ nanocomposite for synergistic eradication of cancer cells via DOX/pCRISPR delivery, Adv. Compos. Hybrid Mater. 7 (1) (2024) 18, https://doi.org/10.1007/s42114-023-00825-y.
[75] Y. Huang, S.P. Cole, T. Cai, Y. Cai, Applications of nanoparticle drug delivery systems for the reversal of multidrug resistance in cancer, Oncol. Lett. 12 (1) (2016) 11–15, https://doi.org/10.3892/ol.2016.4596.
[76] W.J. Lin, W.C. Lee, Polysaccharide-modified nanoparticles with intelligent CD44 receptor targeting ability for gene delivery, Int. J. Nanomedicine (2018) 3989–4002, https://doi.org/10.2147/IJN.S163149.